

# Comparative study of desktop- and synchrotron radiation-based micro computed tomography analyzing cell-seeded scaffolds in tissue engineering of bone

Adam Papadimitropoulos\*<sup>a</sup>, Sebastian Friess<sup>b</sup>, Felix Beckmann<sup>c</sup>, Phil Salmon<sup>d</sup>, Stefania Riboldi<sup>a</sup>, Dietmar Hutmacher<sup>e</sup>, Ivan Martin<sup>a</sup>, and Bert Müller<sup>f</sup>

<sup>a</sup>University Hospital Basel, Basel, Switzerland;

<sup>b</sup>Gloor Instruments AG, Switzerland;

<sup>c</sup>GKSS Research Center, Geesthacht, Germany;

<sup>d</sup>SkyScan NV, Belgium;

<sup>e</sup>Queensland University of Technology, Australia;

<sup>f</sup>Biomaterials Science Center, University of Basel, Switzerland

## ABSTRACT

In the field of tissue engineering, micro computed tomography ( $\mu$ CT) should allow non-destructively assessing the extracellular matrix deposited by cells within porous scaffolds in-vitro. While synchrotron radiation-based  $\mu$ CT combines micrometer resolution with a high signal-to-noise ratio (contrast), recent advances in desktop  $\mu$ CT devices have achieved comparable results with benefits in availability and user-friendliness. In this study we compare the performance of the commercially available, entry-level desktop device 1174 (SkyScan, Belgium) with the  $\mu$ CT at HASYLAB (DESY, Hamburg, Germany) by characterizing porous interconnected 3D scaffolds and monitoring the development of engineered human bone constructs upon culture in such an environment. Expansion of human osteogenic cells has been performed with the use of perfusion bioreactors and 3D scaffolds, serving as cell carriers. Constructs based on low X-ray absorbing, rapid-prototyped fibrous scaffolds were analyzed with a nominal spatial resolution of better than 5  $\mu$ m. Direct 3D image analysis allowed for the accurate quantification of the scaffold morphometry parameters, where both  $\mu$ CT techniques yielded comparable results. However, due to the monochromatic nature of X-rays available at the synchrotron radiation source, drastically reduced beam hardening effects and higher density resolution (higher dynamic range) has been obtained at HASYLAB. Studies in this direction could be useful to highlight the mechanisms that are involved in bone-like tissue growth and to further understand how it can be affected by the choice of cell type, 3D culture environment and scaffold type and architecture.

**Keywords:** micro computed tomography, scaffold, tissue engineering, morphometry, porosity, rigid registration

## 1. INTRODUCTION

More than one million cases of skeletal defects per year require bone-graft procedures to achieve repair and/or regeneration.<sup>1</sup> Current treatments for bone defects include the use of autografts, allografts, and metallic implants.<sup>1-3</sup> Autologous bone grafts are considered as golden standard because of their osteoconductive, osteogenic and osteoinductive properties. Limitation in the quantity, however, harvested from the iliac crest or other sites together with complications observed at the site of surgery, is the main weakness of this method. In addition, autologous bone grafts, have shown considerable resorption and limited viability because of the lack of vascularization.<sup>4</sup> On the other hand, concerns related to the immune response and possible transmission of infectious diseases or lack of osteoconductivity and osteointegration are the main drawbacks that emerge from allografts and metallic implants, respectively.<sup>5</sup> Hence it becomes evident that an adequate bone replacement has yet to be found mastering the mentioned drawbacks. A possible solution may be found from the tissue engineering (TE) field. Bone TE strategies typically consist of combining scaffolds with osteogenic cells, which may offer a potential alternative for the treatment of large clinically challenging bone defects. In this context and in a reductive view, scaffolds are intended as cell delivery vehicles. Such scaffolds,

\*apadimitropoulos@uhbs.ch; phone +41 65 328 73 75; fax +41 61 265 39 90; www.icfs-basel.ch

however, are not only simple bio-inert cell carriers, but they should have the difficult task of driving tissue regeneration in vivo and most importantly, of being informative for cells. In other words, they should direct cell differentiation fate by providing a correct microenvironment and physico-chemical inputs. Scaffold properties such as porosity, pore size, interconnectivity, surface accessible area and strut thickness, respectively, are considered to be essential and have to be fully assessed to make them suitable for TE purposes.<sup>6-11</sup> The scaffold alone is insufficient to regenerate bone tissue in vivo, and thus complementary strategies are employed that make use of osteogenic cells in order to increase the efficacy of the scaffold.<sup>12</sup> When seeded on appropriate scaffolds under suitable culture conditions in vitro, osteogenic cells are capable to proliferate and produce extra-cellular matrix (ECM) which progressively mineralizes to form a bony tissue. Moreover, ECM can act as a storage reservoir for growth factors and release them when necessary.<sup>13,14</sup> A recent study<sup>15</sup> showed that grafts comprised of scaffold together with osteogenic cells stimulated the ECM production. They can positively influence the bone formation efficiency in vivo. Additionally, with the use of perfusion bioreactors which also provide dynamic culture conditions in vitro<sup>16</sup> in highly controllable and reproducible manner, they also give mechanical stimulation to seeded cells in the form of fluid shear stress, resulting in increased deposition of ECM.<sup>17</sup>

An important question is whether an in-vitro generated ECM is sufficiently suited in order to predict the in vivo bone forming potential of an engineered generated graft. Traditional methods of quantifying ECM deposition consist of destructive methods such as collagen-I and calcium measurements<sup>18</sup> impeding any further characterization. Ideally, such a measurement should be non-destructive, non-invasive and three-dimensional, making use of the scaffold's dimensions providing precise quantitative endpoints.<sup>19</sup> Micro computed tomography ( $\mu$ CT) appears to be such a measurement technique. It provides hierarchical biological imaging with isotropic resolution ranging from few millimeters (clinical CT) down to 100 nm (synchrotron radiation-based, SR $\mu$ CT) and even below. SR $\mu$ CT has been already successfully used for quantification of the three-dimensional micro-architecture of bone including engineered bone.<sup>20-22</sup> While SR $\mu$ CT combines micrometer resolution with a high signal-to-noise ratio (contrast), recent advances in desktop  $\mu$ CT devices have achieved comparable results for bony tissues with benefits in availability and user-friendliness.<sup>23-28</sup>

Our ultimate goal is to establish a non-destructive method to assess the ECM deposited by cells within 3D porous constructs, giving us precise quantitative data for optimizing TE processes for generating bone grafts, ideally at clinically relevant dimensions. For practical reasons, such a concept should become feasible taking advantages of desktop  $\mu$ CT instrumentation.

The current study compares the performance of the commercially available, entry-level desktop device 1174 (SkyScan, Belgium) with the SR $\mu$ CT at HASYLAB (DESY, Hamburg, Germany) by characterizing the interconnected porous scaffolds and attempting to monitor the development of engineered human bone constructs upon culture in this 3D environment. Expansion of human osteogenic cells has been performed using the perfusion bioreactors and 3D scaffolds, as previously described.<sup>29</sup> Constructs based on low X-ray absorbing, rapid-prototyped fibrous scaffolds were analyzed with the nominal spatial resolution of better than 5  $\mu$ m. The presented results indicate that the scaffold characterization by means of morphometric analysis can be straightforward and successful with a desktop microCT. ECM monitoring, however, has not yet been successful, even if synchrotron radiation-based instrumentation is used.

## 2. MATERIALS AND METHODS

### 2.1 Scaffold fabrication

The scaffolds with a 0,60,120 degree lay-down pattern were fabricated by fused deposition modeling.<sup>30</sup> Raw materials (medical grade polycaprolactone mPCL from Birmingham polymers, UK, and tricalcium phosphate TCP (80:20) from Rebone Biomaterials Co. Ltd, China) were prepared into  $1.70 \pm 0.10$  mm diameter monofilaments via a filament extrusion process using an in-house built extruder. The mPCL-TCP (20%wt) physical blend was prepared by combining the PCL polymer and TCP in dichloromethane (JT Baker). The mPCL-TCP composition was achieved from optimization studies to develop a suitable composition for usage with the FDM process (data not shown). The FDM 3000 rapid prototyping system from Stratasys Inc. was used to produce the mPCL-TCP scaffolds of a bulk dimensions (fiber diameter 400  $\mu$ m and pore size 300  $\mu$ m x 400  $\mu$ m x 600  $\mu$ m) for ease and efficiency of processing, and subsequently cut into the required sizes for the study (cylinders with 8 mm in diameter and 4 mm high). The scaffold structure composed of polymeric PCL fibers and TCP granules is depicted in figure 1 (3D model). In order to investigate possible ways to optimize cell retention and matrix formation during in vitro cell culture (by increasing the surface/volume ratio available to cells), part of the scaffolds have been pre-coated with a lyophilized type-I collagenous matrix.

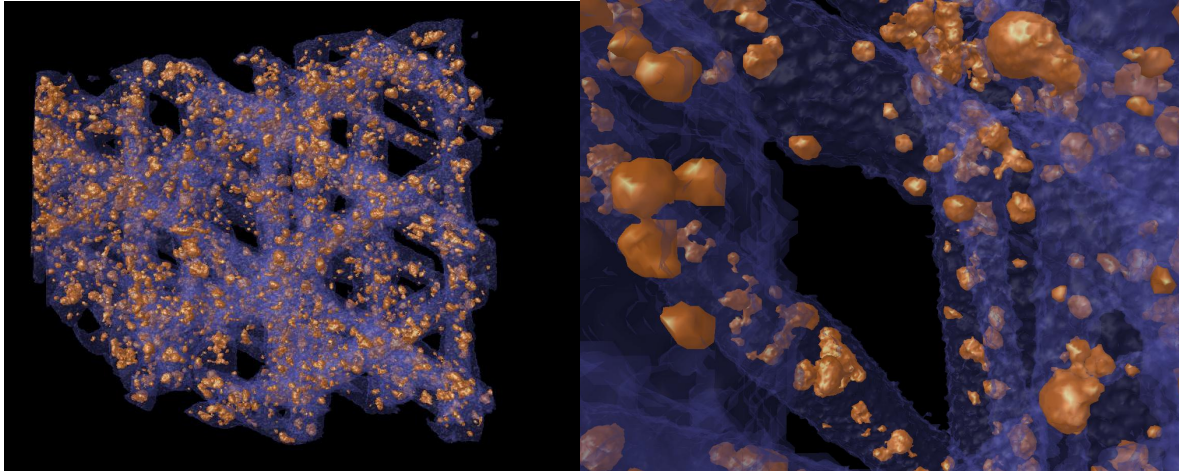


Fig. 1. 3D visualizations of a PCL-TCP scaffold using the desktop  $\mu$ CT 1174 and the software CT-Analyzer and CT-Vol, all from SkyScan NV, Belgium. The PCL fibre network is easily distinguishable from the small embedded TCP particles.

## 2.2 In-vitro experiments

Bone marrow aspirates (20- to 40-ml volumes) were obtained from healthy donors (36–54 years old) during routine orthopedic surgical procedures in accordance with the local ethical committee (University Hospital Basel) and after informed consent. Nucleated cells were isolated from aspirates using a red blood cells lysis buffer. Cell seeding and subsequent culture of freshly isolated cells from bone marrow in 3D scaffolds were performed using a previously described bioreactor system,<sup>31</sup> which is based on the principle of continuous direct perfusion of cell suspensions or culture medium through the pores of 3D scaffolds in alternate directions. Bone marrow cells ( $15 \times 10^6$  cells per scaffold) were perfused at a velocity of 1.2 ml/min through the mPCL-TCP scaffolds in a medium ( $\alpha$ -modified Eagle's medium containing 10% fetal bovine serum supplemented with 5 ng/ml fibroblast growth factor-2, 10 nM dexamethasone, and 0.1 mM L-ascorbic acid-2-phosphate) to increase osteogenic cell proliferation and give osteogenic commitment to them. After 5 days, the initial cell suspension was completely removed and replaced by fresh medium. The cell-scaffold constructs were perfused for an additional 14 days (cell expansion phase) at a velocity of 0.3 ml/min (previously determined to support cell viability throughout the scaffold thickness), with medium changes twice a week. Figure 2 shows the experimental outline used to generate the cell-scaffold constructs in the perfusion bioreactor. At the end of culture, the generated constructs were fixed in 4% formalin overnight, and then washed and kept in phosphate buffered saline (PBS) at 4 °C for  $\mu$ CT analysis. Moreover, scaffolds that served as duplicates were stained with MTT (3-(4,5-Dimethyl-2-thiazolyl)-2,5-diphenyltetrazolium bromide) to have a qualitative assessment of cell viability and distribution. Briefly, cell-scaffold constructs were placed onto 6-multiwell plates and washed twofold with PBS at the temperature of 37 °C. Subsequently, they were incubated for 120 min at 37 °C with 3 ml per well of a freshly prepared MTT solution (0.1% w/v): MTT in Dublecco's medium, without phenol red, and supplemented with HEPES. Then, they have been washed again twice and left in PBS. Pictures of these scaffolds were acquired by a 3D stereo light microscope and are shown in figure 3.

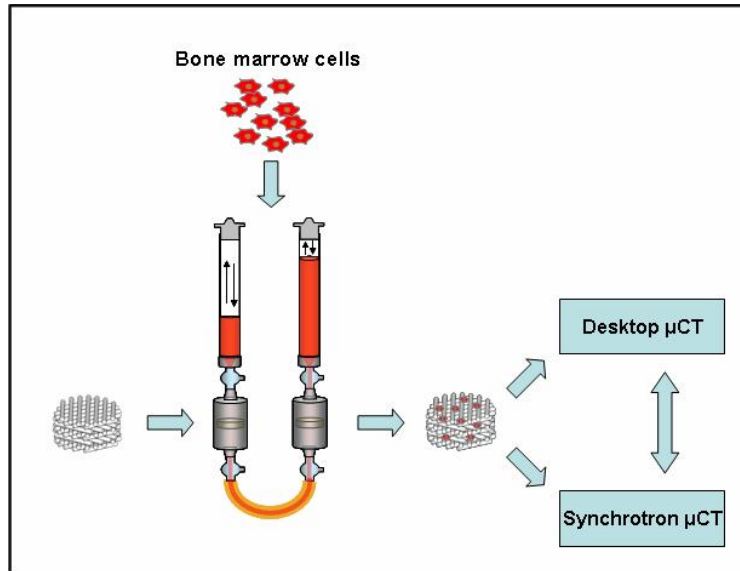


Fig. 2. Experimental outline used to generate the cell-scaffold constructs in a perfusion bioreactor system allowing to perform comparative studies between the selected tomography set-ups.

### 2.3 SR $\mu$ CT measurements

The SR $\mu$ CT data were acquired in absorption contrast mode at the beamline BW 2, which has been operated by GKSS-Research Center at HASYLAB / DESY Hamburg, Germany.<sup>32</sup> Using the photon energy of 19 keV, the projections acquired contained 1536 x 1024 pixels, which corresponded to the pixel length of 4.8  $\mu$ m and, hence, a field of view of 7.4 x 4.9 mm<sup>2</sup>. The spatial resolution of system was determined to be 8.5  $\mu$ m by means of the modulation transfer function.<sup>33</sup> The 3D datasets were reconstructed taking advantage of the standard filtered back-projection reconstruction algorithm out of 721 projections.<sup>34</sup> For easier registration, the dataset was reduced by the factor of 27 (isotropic 3-fold binning) prior to reconstruction, which also gives rise to improved contrast.<sup>35</sup> As the different scaffolds were larger than the field of view or exhibited bubble formation, they were only partially acquired.

### 2.4 Desktop $\mu$ CT measurements

The desktop  $\mu$ CT data were acquired on a SkyScan 1174 table top scanner (SkyScan NV, Kontich, Belgium) with using unfiltered X-rays at an applied voltage of 50 kV and a current of 800  $\mu$ A. Transmission images were acquired for a 180 degrees scan rotation with an incremental rotation step size of 0.4 degrees. Reconstruction was made with a modified Feldkamp algorithm at an isotropic voxel size of 7.18  $\mu$ m. From the reconstruction results, it was possible to calculate 3D objects with the use of an external program (CT-Analyzer and CT-Volume, both SkyScan NV). After completion of the scanning procedure, we replaced the samples in the saline solution.

### 2.5 Tomogram analysis

In order to obtain comparable quantitative results for the tomograms acquired from SkyScan 1174 and SR $\mu$ CT the common volume has to be extracted after reliable rigid registration. The affine registration algorithm applied was based on nine independent parameters, i.e. three translational, three rotational and three scaling degrees of freedom, respectively. Appropriate starting parameters for the automatic rigid registration were manually found by means of the numerous characteristic features in the tomography data. Here, user-based IDL-code was developed to choose three non-collinear feature-based landmarks in both tomograms and to reveal the parameters for the coordination transform.

The subsequently applied automatic registration algorithm relates to the non-rigid matching based on the classical maximization of the mutual information.<sup>36,37</sup> The nine registration parameters were determined by the Powell multidimensional search<sup>38</sup> such that the mutual information between the SR $\mu$ CT-reference dataset and the SkyScan  $\mu$ CT-data was maximized.

Morphometric parameters of the scaffold PCL fibers and of TCP granules within fibers were carried out with SkyScan CT-analyser software using conditional binary operations. Among others, the determined parameters were: total VOI volume TV, object volume Obj.V, percent object volume Obj.V/TV, object surface Obj.S, object surface/volume ratio Obj.S/Obj.V, structure thickness St.Th, and structure model index SMI, respectively. The same analysis was carried out on both datasets derived from the SR $\mu$ CT and from the portable desktop SkyScan 1174  $\mu$ CT after registration and extraction of the common volume-of-interest described above. Binary threshold values were selected to segment the scaffold from the liquid medium in the Eppendorf tube. Subsequently, the scaffold was subdivided into the highly absorbing TCP granules and the lower absorbing PCL fibers also by intensity-based thresholding.

In the morphometric analysis, some of the volume-referenced parameters critically depend on the selected volume of interest. Therefore, three morphometric approaches were carried out. The first one analyzed the polymer components relative to the tube contents. The second one determined the parameters of the calcified deposits with respect to the polymer. The third approach also determined the parameters of the calcified deposits but with respect to the tube contents as the reference volume. We here compare the parameters of the first and the third volumetric references, thus the tube content was always selected as the reference volume (total VOI volume TV). This simplification is feasible, since all datasets were pre-registered in order to retrieve comparable volumes of interest.

An automated batch analysis procedure was run in order to obtain the scaffold characteristic parameters. Based on the volume selection and the scaffold binarization, noise was removed by despeckling and object removal smaller than 40 voxels. In order to solidify the structure, dilatation and erosion using one voxel size was carried out. Subsequently, the noise inside the structure was removed again by despeckling and removal of voids smaller than 40 voxels. These data provided the basis of the extraction of the scaffold morphology from the other components. Applying an appropriate threshold on the original grayscale values within the scaffold, the TCP granules were extracted also by binarization and noise reduction (despeckling and removal of objects smaller than 20 voxels). Consequently, the morphometry of the TCP became too light.

### 3. RESULTS AND DISCUSSION

At the end of the culture period, cells viability was determined for both scaffold types by MTT staining. The reduction of MTT to purple color is catalyzed by mitochondrial dehydrogenases. The intensity of the staining is correlated to the viability of the cells. In the present study, both scaffold types were positive for MTT indicating the presence of viable cells. Moreover, cells were distributed not only across the fibers of the scaffolds, but also in their pores. The latter means that independently of the pre-coating to the scaffolds with collagen, cells could proliferate even in the pore's center indicating the presence of ECM matrix, which in turn provided support to the cells to be expanded. The results from MTT staining are depicted in figure 3.



Fig. 3. The optical micrographs show the bare PCL-TCP scaffold (left) and the collagen-I pre-coated PCL-TCP scaffold (right) after the MTT staining of the 19-days cell culture using the 3D perfusion bioreactor system.

Duplicates of the above experiment were appropriately processed and analyzed for  $\mu$ CT as explained above. Quantitative data related to the morphometric parameters important for scaffold TE are summarized in the Table 1.

Table. 1. Morphometric analysis of the PCL polymeric fibers (low density) and the embedded TCP granules (high density) for the two scaffold types derived from SkyScan 1174 and SR $\mu$ CT devices.

	PCL-TCP coated with col-I (low density)							PCL-TCP coated with col-I (high density)						
	TV mm <sup>3</sup>	Obj.V mm <sup>3</sup>	Obj.V/TV %	Obj.S mm <sup>2</sup>	Obj.S/Obj.V 1/mm	St.Th mm	SMI	TV mm <sup>3</sup>	Obj.V mm <sup>3</sup>	Obj.V/TV %	Obj.S mm <sup>2</sup>	Obj.S/Obj.V 1/mm	St.Th mm	SMI
$\mu$ CT	65.6	11.6	17.7	187	16.1	0.28	2.31	65.6	0.52	0.80	42.6	81.1	0.072	3.77
SR $\mu$ CT	62.6	11.0	17.5	184	16.8	0.28	3.57	62.4	0.47	0.76	59.6	126	0.056	3.64

	PCL-TCP (low density)							PCL-TCP (high density)						
	TV mm <sup>3</sup>	Obj.V mm <sup>3</sup>	Obj.V/TV %	Obj.S mm <sup>2</sup>	Obj.S/Obj.V 1/mm	St.Th mm	SMI	TV mm <sup>3</sup>	Obj.V mm <sup>3</sup>	Obj.V/TV %	Obj.S mm <sup>2</sup>	Obj.S/Obj.V 1/mm	St.Th mm	SMI
$\mu$ CT	65.0	8.96	1.38	151	16.8	0.27	2.31	65.0	0.40	0.62	32	80.8	0.071	3.78
SR $\mu$ CT	62.7	8.35	1.33	131	15.7	0.28	2.44	62.7	0.37	0.60	47	126.0	0.051	3.66

The morphometric analysis did not yield significant differences between the SkyScan 1174 and the SR $\mu$ CT systems for the fibrous scaffold structure. Moderate declinations occur analyzing small structures as the TCP granules. The results, however, demonstrate that even the rather simple desktop  $\mu$ CT allows extracting meaningful data of rather complex and even lower X-ray absorbing structures and therefore yield quantitative images to optimize 3D scaffolds for TE purposes.

Volume histograms, i.e. the voxel frequency distribution over the 256 gray levels from desktop  $\mu$ CT datasets, are depicted in figure 4. Four distinct peaks are identified, which correspond (from left to right) to surrounding air, Eppendorf tube, watery environment (PBS) and the fibrous scaffold structure. The TCP granules exhibit a broad peak of low intensity at much higher gray values (not shown in figure 4). According to low absorption coefficient of the collagenous ECM matrix formed by cells that is comparable to the one of PBS, it is hypothesized that ECM resides in the third peak in the histogram. It was, however, impossible to distinguish between ECM and PBS using the SkyScan desktop system. Moreover, no significant difference has been observed between the histograms of the two scaffold types.

Comparatively, figure 5 shows the related volume histograms of the local absorption coefficients derived from the SR $\mu$ CT data of the two scaffolds. In order to increase the density resolution (contrast), the projection images were binned in steps of integers up to the binning factor of 3 prior to tomographic reconstruction.<sup>35</sup> For the higher binning factors the peaks become clearer and steeper that facilitated the segmentation of the different components. As shown above for the desktop system, the peaks correspond to surrounding air, Eppendorf tube, watery environment (PBS) and the fibrous scaffold structure. The binning procedure should especially help to identify further components within the PBS. Unfortunately, it was impossible to identify the ECM even by means of the synchrotron radiation-based monochromatic tomography. It should also be noted that no evident differences were observed between the histograms for the two scaffold types.

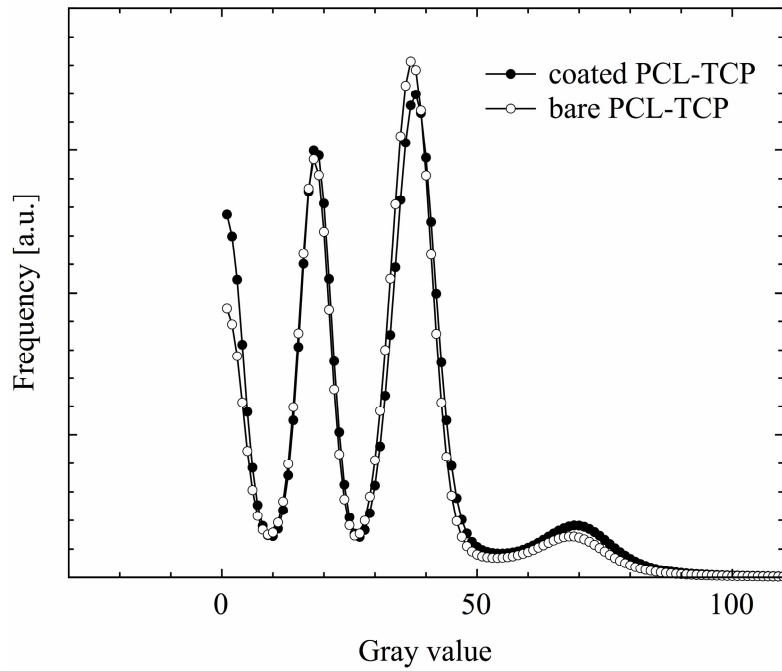


Fig. 4. Volume histograms derived from the desktop SkyScan 1174 obtained for the two scaffolds investigated. Peaks correspond (from left to right) to surrounding air, Eppendorf tube, watery environment (PBS) and the fibrous scaffold structure. The TCP granules exhibit a broad peak of low intensity at much higher gray values (not shown).

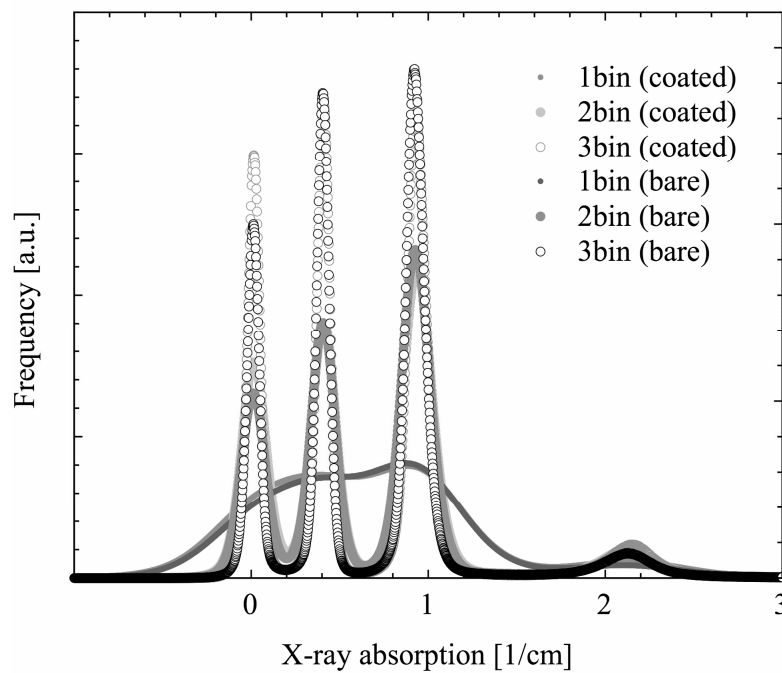


Fig. 5. The X-ray absorption histograms of SR $\mu$ CT data for the two scaffold types are almost identical. The application of the binning factors of 1, 2, and 3 to the projection data prior to the reconstruction reveals significant improvement of the density resolution, which facilitates the segmentation of the different components.

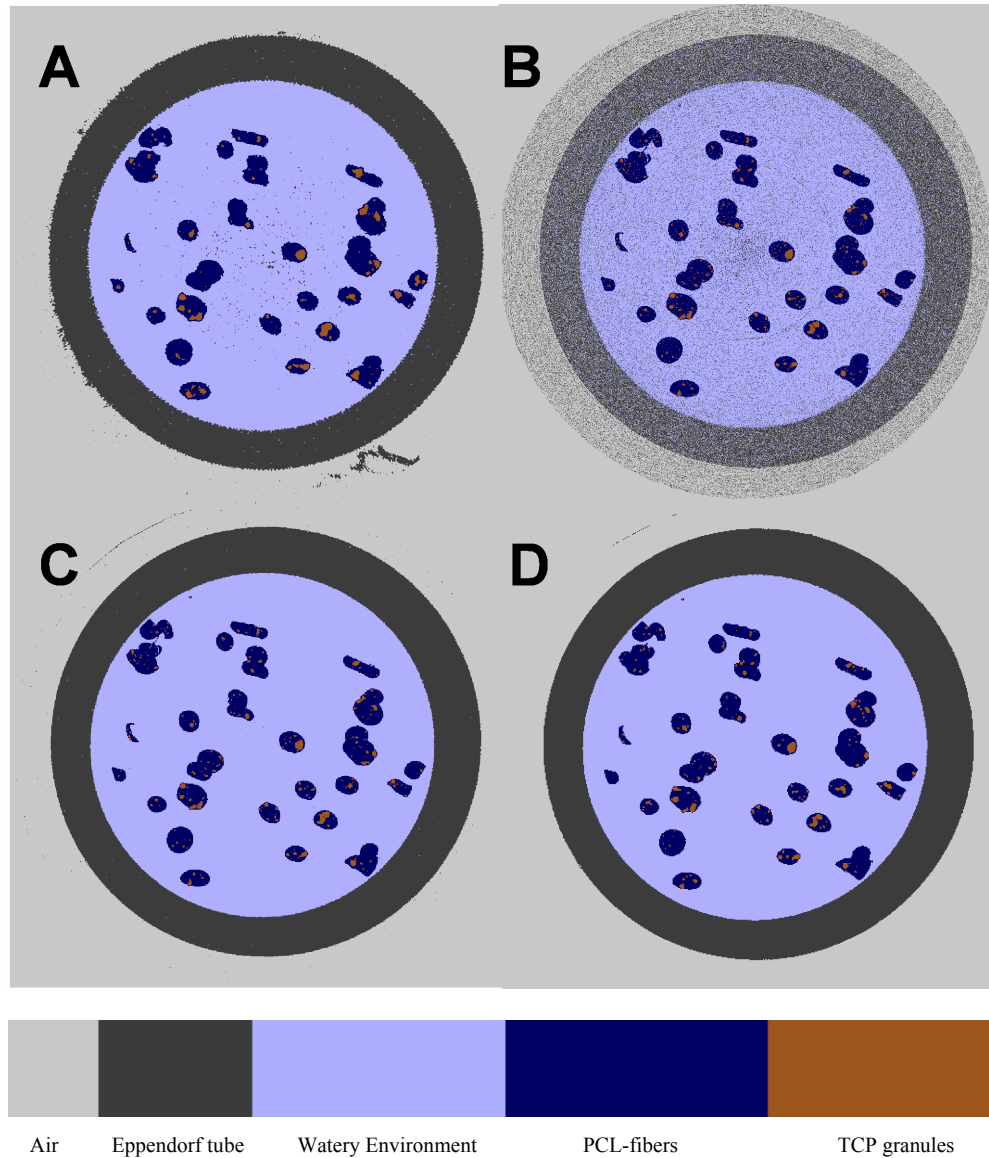


Fig. 6. The selected tomographic slice qualitatively demonstrates the density resolution in the different datasets. A: desktop  $\mu$ CT, B – D: SR $\mu$ CT for the binning factors 1, 2, and 3, respectively.

Figure 6 represents four tomography slices of the identical region (registered data). The colors selected according to the gray values or the local absorption values support identifying the different components namely surrounding air, Eppendorf tube, PBS including cells and ECM, PCL fibers and larger TCP particles. Interestingly, even the entry-level desktop  $\mu$ CT permits the identification of all larger components. There are only very few exceptions related to the smallest entities. Appropriate calibration of the desktop  $\mu$ CT should therefore allow transforming the gray values to absorption coefficients, which could help to identify the chemical nature of the individual phases.

In this study we compared the performance of the commercially available desktop  $\mu$ CT 1174 (SkyScan, Belgium) with the SR $\mu$ CT facilities at HASYLAB (DESY, Hamburg, Germany) characterizing the interconnected porous, cell seeded scaffolds to monitor the development of engineered human bone constructs upon culture in 3D environment. Such an approach could be very supportive for the quality control of TE-constructs and for the optimization of culturing conditions.

Unfortunately, both the conventional desktop as well as the synchrotron radiation-based  $\mu$ CT failed to monitor the ECM produced by the cells, although the MTT assay showed the presence of the gel-like tissue, which hold the cells away from the surfaces of the fibrous scaffolds. This tissue exhibited the same X-ray absorption as PBS. Therefore, one has to increase or decrease the X-ray absorption adding or replacing certain species. The application of sophisticated software tools as the improvement of the density resolution by the binning of the projection images seems to be less successful to identify any trace of the ECM. A higher degree of ECM mineralization might be the key to identify and segment the ECM from the surrounding liquid. The medium used for the cell cultures was chosen to give an osteogenic commitment to the cells and not to highly stimulate their differentiation. The reason was to maintain their stem-like status as much as possible. Moreover, this choice of medium has been demonstrated earlier<sup>29</sup> to give rise to grafts that can form bone, once implanted in-vivo, in a robust and reproducible manner.

It is well known that staining agents, such as  $\text{OsO}_4$  or gold significantly enhance the contrast of the low-absorbing cells and ECM tissue. Such staining methods, however, are usually regarded to be destructive, since the toxic species are harmful to the viability of the cells. Here, nontoxic agents such as lipiodol may offer an alternative, as already shown in particular human radiological investigations.<sup>39</sup>

The successful segmentation of the scaffold and the differentiation of the scaffold's components allowed for the quantitative analysis of the scaffold morphology at micrometer resolution. The morphometric analysis well known from trabecular bone analysis can be meaningfully applied not only to the SR $\mu$ CT but also to the conventional desktop  $\mu$ CT datasets. More sophisticated procedures<sup>11</sup> may also be applied to further characterize our TE constructs, since data quality from both techniques was high enough. The rather complex morphology of the different components of the specimens is a prominent example that commercially available  $\mu$ CT systems are already very supportive to optimize the system of interest such as scaffolds in TE. Only few comparative measurements with monochromatic X-rays are necessary to calibrate the conventional  $\mu$ CT data and to validate them. Such an approach also accounts for the limited beamtime at synchrotron radiation sources. The better accessibility and user-friendliness makes today's desktop CT systems an important instrument in the TE laboratory for the quantitative characterization of customized scaffolds fabricated for example by rapid prototyping techniques to repair patient-specific defects caused by accidents, tumor surgery etc. In this context, the desktop  $\mu$ CT-systems in the lab can be efficiently used to preselect dedicated specimens out of the numerous constructs for subsequent SR-based  $\mu$ CT experiments.

## ACKNOWLEDGMENTS

The authors acknowledge HASYLAB at DESY (Hamburg, Germany) for providing beamtime in the frame of the approved proposal I-05-028. This work is partially funded by the European Space Agency program 14232/00/NL/SH through the ERISTO project.

## REFERENCES

- [1] Yaszemski M.J., Oldham J.B., Lu L., and Currier B.L., [Bone Engineering], 1st Edition, Em Squared ed 1994, p. 541.
- [2] H. Hatano, A. Ogoe, T. Hotta, N. Endo, H. Umezu, and T. Morita, "Extracorporeal irradiated autogenous osteochondral graft: a histological study," *J. Bone Joint Surg. Br.*, 87(7), pp. 1006-1011, July2005.
- [3] C. R. Perry, "Bone repair techniques, bone graft, and bone graft substitutes," *Clin. Orthop. Relat Res.*,(360), pp. 71-86, Mar.1999.
- [4] G. L. Le, P. Layrolle, and G. Daculsi, "A review of bioceramics and fibrin sealant," *Eur. Cell Mater.*, 8, pp. 1-10, 2004.
- [5] W. L. Fodor, "Tissue engineering and cell based therapies, from the bench to the clinic: the potential to replace, repair and regenerate," *Reprod. Biol. Endocrinol.*, 1, p. 102, Nov.2003.
- [6] C. M. Agrawal and R. B. Ray, "Biodegradable polymeric scaffolds for musculoskeletal tissue engineering," *J. Biomed. Mater. Res.*, 55(2), pp. 141-150, May2001.
- [7] D. W. Hutmacher, "Scaffolds in tissue engineering bone and cartilage," *Biomaterials*, 21(24), pp. 2529-2543, Dec.2000.

- [8] K. F. Leong, C. M. Cheah, and C. K. Chua, "Solid freeform fabrication of three-dimensional scaffolds for engineering replacement tissues and organs," *Biomaterials*, 24(13), pp. 2363-2378, June2003.
- [9] G. Vunjak-Novakovic and L. E. Freed, "Culture of organized cell communities," *Adv. Drug Deliv. Rev.*, 33(1-2), pp. 15-30, Aug.1998.
- [10] S. Yang, K. F. Leong, Z. Du, and C. K. Chua, "The design of scaffolds for use in tissue engineering. Part I. Traditional factors," *Tissue Eng*, 7(6), pp. 679-689, Dec.2001.
- [11] F. C. Fierz, F. Beckmann, M. Huser, S. H. Irsen, B. Leukers, F. Witte, O. Degistirici, A. Andronache, M. Thie, and B. Muller, "The morphology of anisotropic 3D-printed hydroxyapatite scaffolds," *Biomaterials*, 29(28), pp. 3799-3806, Oct.2008.
- [12] A. I. Caplan and S. P. Bruder, "Mesenchymal stem cells: building blocks for molecular medicine in the 21st century," *Trends Mol. Med.*, 7(6), pp. 259-264, June2001.
- [13] P. Bashkin, S. Doctrow, M. Klagsbrun, C. M. Svahn, J. Folkman, and I. Vlodavsky, "Basic fibroblast growth factor binds to subendothelial extracellular matrix and is released by heparitinase and heparin-like molecules," *Biochemistry*, 28(4), pp. 1737-1743, Feb.1989.
- [14] E. Schonherr and H. J. Hausser, "Extracellular matrix and cytokines: a functional unit," *Dev. Immunol.*, 7(2-4), pp. 89-101, 2000.
- [15] H. Castano-Izquierdo, J. varez-Barreto, D. J. van den, J. A. Jansen, A. G. Mikos, and V. I. Sikavitsas, "Pre-culture period of mesenchymal stem cells in osteogenic media influences their in vivo bone forming potential," *J. Biomed. Mater. Res. A*, 82(1), pp. 129-138, July2007.
- [16] X. Yu, E. A. Botchwey, E. M. Levine, S. R. Pollack, and C. T. Laurencin, "Bioreactor-based bone tissue engineering: the influence of dynamic flow on osteoblast phenotypic expression and matrix mineralization," *Proc. Natl. Acad. Sci. U. S. A*, 101(31), pp. 11203-11208, Aug.2004.
- [17] V. I. Sikavitsas, G. N. Bancroft, H. L. Holtorf, J. A. Jansen, and A. G. Mikos, "Mineralized matrix deposition by marrow stromal osteoblasts in 3D perfusion culture increases with increasing fluid shear forces," *Proc. Natl. Acad. Sci. U. S. A*, 100(25), pp. 14683-14688, Dec.2003.
- [18] V. I. Sikavitsas, G. N. Bancroft, J. J. Lemoine, M. A. Liebschner, M. Dauner, and A. G. Mikos, "Flow perfusion enhances the calcified matrix deposition of marrow stromal cells in biodegradable nonwoven fiber mesh scaffolds," *Ann. Biomed. Eng*, 33(1), pp. 63-70, Jan.2005.
- [19] G. H. van Lenthe, H. Hagenmuller, M. Bohner, S. J. Hollister, L. Meinel, and R. Muller, "Nondestructive micro-computed tomography for biological imaging and quantification of scaffold-bone interaction in vivo," *Biomaterials*, 28(15), pp. 2479-2490, May2007.
- [20] V. S. Komlev, F. Peyrin, M. Mastrogiacomo, A. Cedola, A. Papadimitropoulos, F. Rustichelli, and R. Cancedda, "Kinetics of in vivo bone deposition by bone marrow stromal cells into porous calcium phosphate scaffolds: an X-ray computed microtomography study," *Tissue Eng*, 12(12), pp. 3449-3458, Dec.2006.
- [21] M. Mastrogiacomo, A. Papadimitropoulos, A. Cedola, F. Peyrin, P. Giannoni, S. G. Pearce, M. Alini, C. Giannini, A. Guagliardi, and R. Cancedda, "Engineering of bone using bone marrow stromal cells and a silicon-stabilized tricalcium phosphate bioceramic: evidence for a coupling between bone formation and scaffold resorption," *Biomaterials*, 28(7), pp. 1376-1384, Mar.2007.
- [22] A. Papadimitropoulos, M. Mastrogiacomo, F. Peyrin, E. Molinari, V. S. Komlev, F. Rustichelli, and R. Cancedda, "Kinetics of in vivo bone deposition by bone marrow stromal cells within a resorbable porous calcium phosphate scaffold: an X-ray computed microtomography study," *Biotechnol. Bioeng.*, 98(1), pp. 271-281, Sept.2007.
- [23] K. Balto, R. Muller, D. C. Carrington, J. Dobeck, and P. Stashenko, "Quantification of periapical bone destruction in mice by micro-computed tomography," *J. Dent. Res.*, 79(1), pp. 35-40, Jan.2000.
- [24] R. E. Guldberg, A. S. Lin, R. Coleman, G. Robertson, and C. Duvall, "Microcomputed tomography imaging of skeletal development and growth," *Birth Defects Res. C. Embryo. Today*, 72(3), pp. 250-259, Sept.2004.
- [25] R. Muller, T. Hildebrand, H. J. Hauselmann, and P. Rueggsegger, "In vivo reproducibility of three-dimensional structural properties of noninvasive bone biopsies using 3D-pQCT," *J. Bone Miner. Res.*, 11(11), pp. 1745-1750, Nov.1996.
- [26] R. Muller, M. Hahn, M. Vogel, G. Delling, and P. Rueggsegger, "Morphometric analysis of noninvasively assessed bone biopsies: comparison of high-resolution computed tomography and histologic sections," *Bone*, 18(3), pp. 215-220, Mar.1996.
- [27] E. Tanck, J. Homminga, G. H. van Lenthe, and R. Huiskes, "Increase in bone volume fraction precedes architectural adaptation in growing bone," *Bone*, 28(6), pp. 650-654, June2001.

- [28] T. Yamashita, Y. Nabeshima, and M. Noda, "High-resolution micro-computed tomography analyses of the abnormal trabecular bone structures in klotho gene mutant mice," *J. Endocrinol.*, 164(2), pp. 239-245, Feb.2000.
- [29] A. Braccini, D. Wendt, C. Jaquiery, M. Jakob, M. Heberer, L. Kenins, A. Wodnar-Filipowicz, R. Quarto, and I. Martin, "Three-dimensional perfusion culture of human bone marrow cells and generation of osteoinductive grafts," *Stem Cells*, 23(8), pp. 1066-1072, Sept.2005.
- [30] D. W. Hutmacher, T. Schantz, I. Zein, K. W. Ng, S. H. Teoh, and K. C. Tan, "Mechanical properties and cell cultural response of polycaprolactone scaffolds designed and fabricated via fused deposition modeling," *J. Biomed. Mater. Res.*, 55(2), pp. 203-216, May2001.
- [31] D. Wendt, A. Marsano, M. Jakob, M. Heberer, and I. Martin, "Oscillating perfusion of cell suspensions through three-dimensional scaffolds enhances cell seeding efficiency and uniformity," *Biotechnol. Bioeng.*, 84(2), pp. 205-214, Oct.2003.
- [32] F. Beckmann, Donath T., Fischer J., Dose T., Lippmann T., and Lottermoser R. et al., "New developments for synchrotron-radiation-based microtomography at DESY," In: Bonse U, editor. *Developments in X-Ray tomography V*, 2006, San Diego:SPIE, 2006.
- [33] B. Muller, F. Beckmann, M. Huser, F. Maspero, G. Szekely, K. Ruffieux, P. Thurner, and E. Wintermantel, "Non-destructive three-dimensional evaluation of a polymer sponge by micro-tomography using synchrotron radiation," *Biomol. Eng.*, 19(2-6), pp. 73-78, Aug.2002.
- [34] A.C. Kak and M. Slaney, [Principles of computerized tomographic imaging]. Philadelphia: SIAM, 2001.
- [35] P. Thurner, F. Beckmann, and B. Muller, "An optimization procedure for spatial and density resolution in hard X-ray micro-computed tomography," *Nucl Instrum Meth Phys Res B*, 225(4), pp. 599-603, 2004.
- [36] F. Maes, A. Collignon, D. Vandermeulen, G. Marchal, and P. Suetens, "Multi-modality image registration by maximization of mutual information," *Mathematical Methods in Biomedical Image Analysis*, pp. 14-22, 1996.
- [37] P. Viola and W. M. Wells, "Alignment by maximization of mutual information," *Fifth International Conference on Computer Vision*, IEEE Computer Society, 1995.
- [38] W. H. Press, B. P. Flannery, S. A. Teukolsky, and W. T. Vetterling, [The Art of Scientific Computing] Cambridge University Press, 1988.
- [39] R. Müller, S. Matter, P. Neuenschwander, U. V. Suter, and P. Rügsegger, "3D micro-tomographic imaging and quantitative morphometry for the nondestructive evaluation of porous biomaterials.," *Morphological Control in Multiphase Polymer Mixtures*, *Mat Res Soc*, 461, pp. 217-221, 1997.